Electronic Supplementary Material (ESI) for Physical Chemistry Chemical Physics.
This journal is © the Owner Societies 2017

Supplementary Information: The structures of liquid pyridine and naphthalene: the effects of heteroatoms and core size on aromatic interactions

S1. Real-space pair correlation functions from Fourier transform of data.

Figures 1 and 2 below show the real space pair correlation functions for samples of pyridine and naphthalene, calculated from Fourier transform of the scattering data (points) and calculated from EPSR simulation (lines). The fit the data is very good. Most of the detail in the f(r) is due to intramolecular structure, the fit therefore a good measure of the (fixed) molecular structure used in the EPSR simulation i.e. bond lengths, angle and dihedrals.

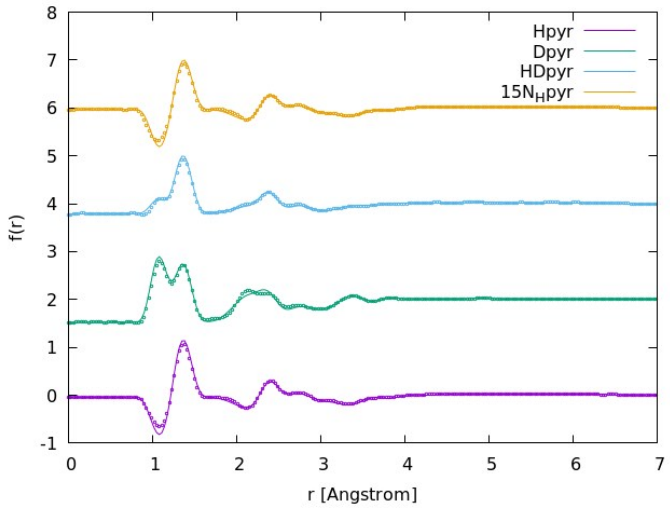

Figure 1: Real-space pair correlation function for four isotopic variants of liquid pyridine. Points are FT of data line is calculated from EPSR simulation.

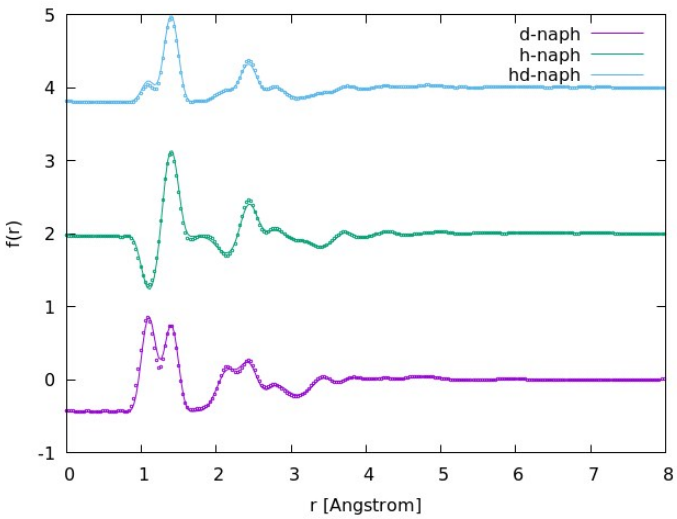

Figure 2: Real-space pair correlation function for three isotopic variants of liquid naphthalene. Points are FT of data line is calculated from EPSR simulation.

S2. Angular radial distribution functions for alternative EPSR simulations of liquid pyridine

Figure 3 shows the angular radial distribution functions for liquid pyridine without refinement to the data (a), without refinement with variation in partial charges (b-c) and after refinement with different partial charges (d-e). These shows how the relatively low level of parallel nearest neighbour contacts, as a small shoulder in the g(r,θ) is a robust feature of the data.

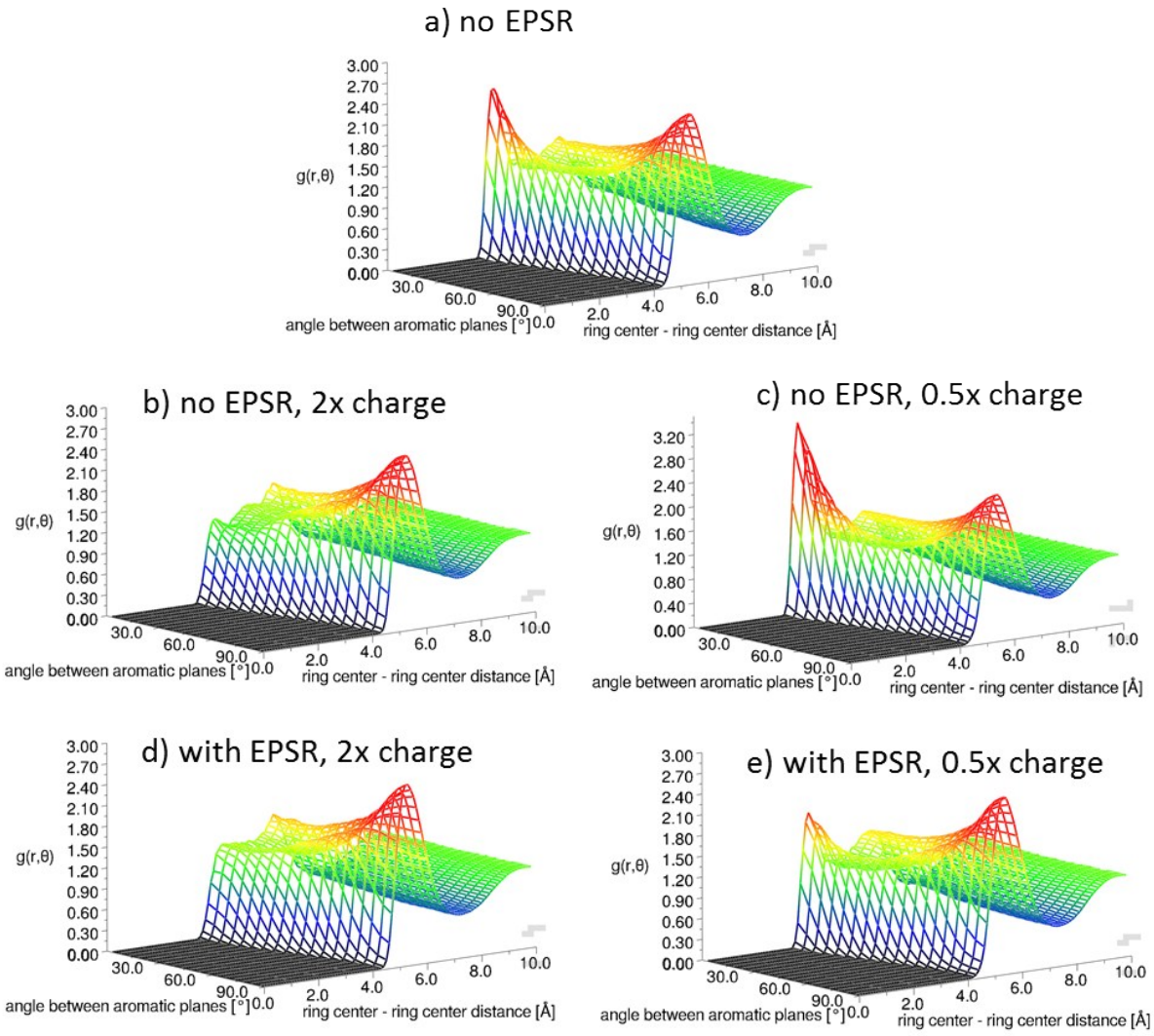

Figure 3: Angular radial distribution functions, calculated as described within the main manuscript, for difference EPSR simulations of liquid pyridine, with different partial charges for seed potentials and with and without refinement to the data

S3. Spatial distribution of hydrogen in liquid pyridine

Figure 4 shows the spatial density function of ortho (H1) and para (H3) hydrogens around a central pyridine molecule, showing a similar preference for the nitrogen atom as seen for the meta (H2) hydrogen. Figure 5 shows the partial g(r) for all three N-H correlations showing a weak peak at ~3Å, much higher than a standard cut-off for hydrogen bonding of 2.5Å

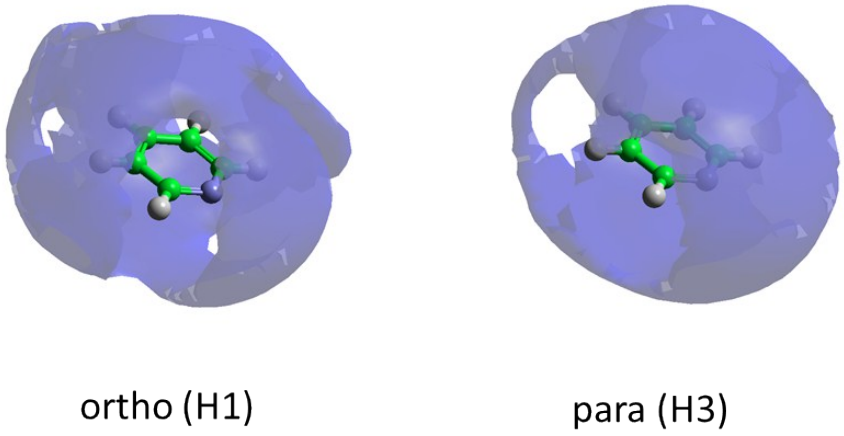

Figure 4: Spatial density functions for ortho (H1) and para (H3) hydrogens around a central pyridine molecule

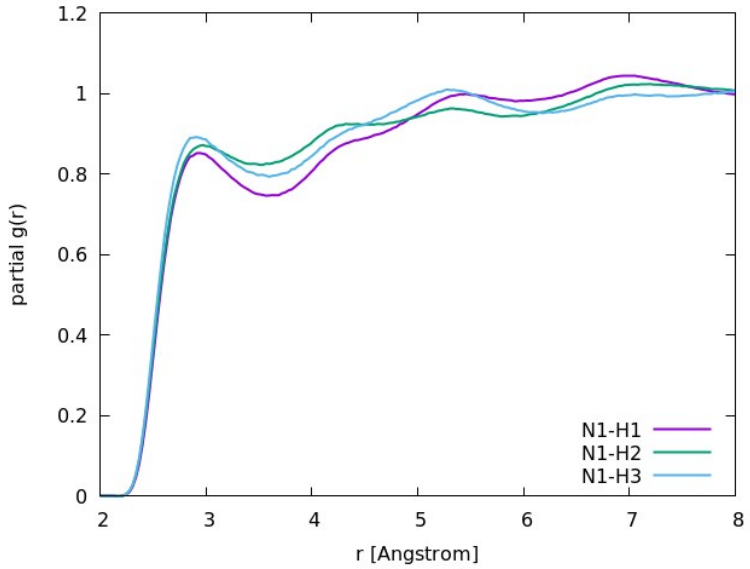

Figure 5: N-H partial g(r)'s from EPSR simulation of liquid pyridine, showing a weak N-H correlation at ~3Å

S4: EPSR simulations of liquid naphthalene with alternative partial charges.

Figure 6 shows the angular radial distribution functions for EPSR simulations of liquid naphthalene with alternative atom-centred partial charges. The upper plots are without refinement to the data, showing how increasing the partial charge removes parallel nearest neighbour contacts and decreasing the charge intensifies them. Refining both of these to the neutron scattering data reproduces a very similar angular radial distribution function. Indicating that this structural feature is well weighted in the data. The alteration of partial charge on the seed potentials does not adversely alter the quality of the fit to the data as shown in Figure 7

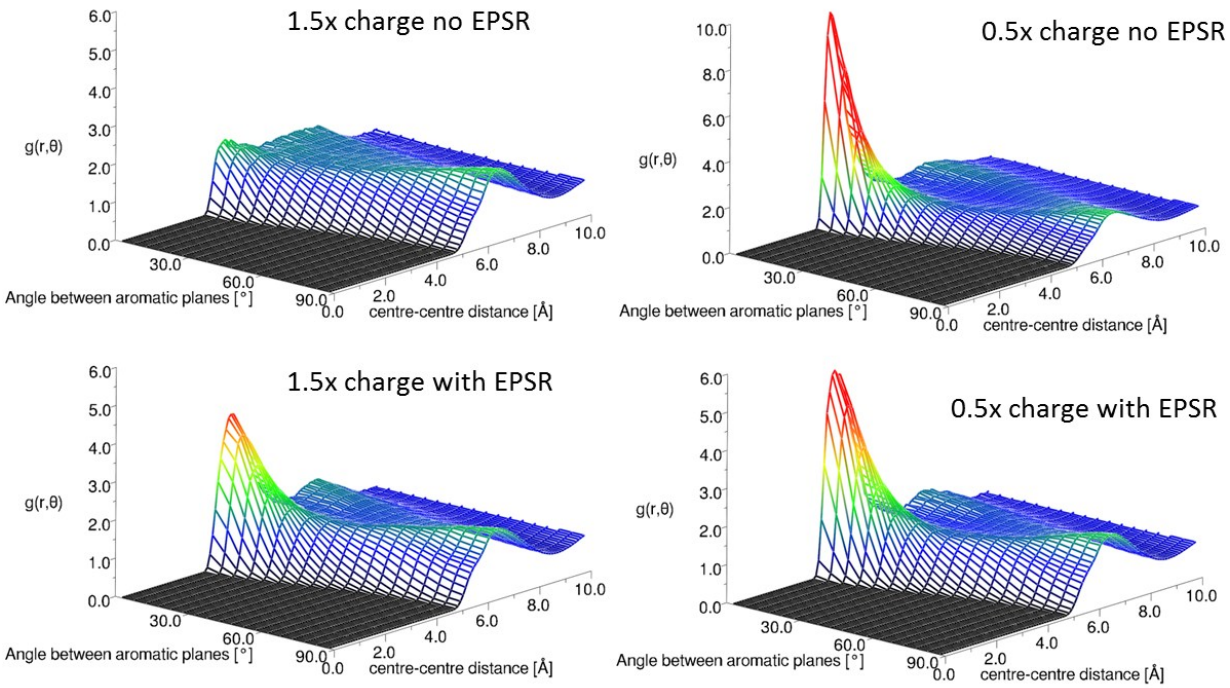

Figure 6: Angular radial distribution functions from Monte Carlo simulations of liquid naphthalene with differing partial charges as the seed potentials (factor of 1.5 or 0.5 of calculated values) and with and without EPSR refinement.

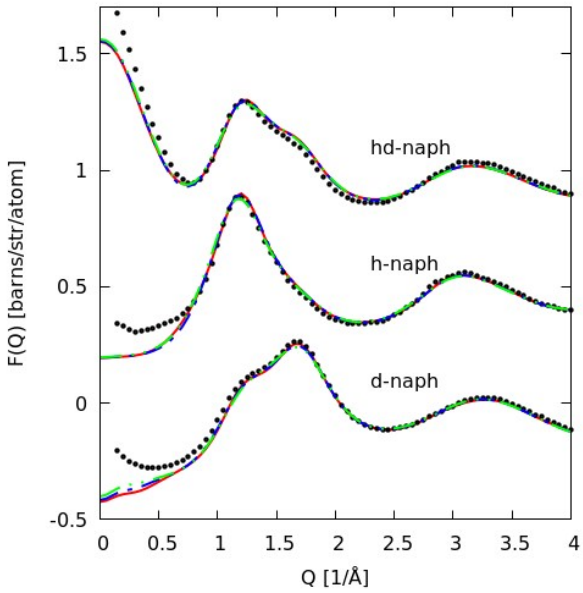

Figure 7: EPSR fit the corrected interference differential scattering cross section (black dots) for EPSR refinements using different seed potentials. Normal seed potential with MOPAC calculated partial charges (red), partial charges increased by factor 1.5 (blue), partial charges decreased by factor 0.5 (green)

S5. Details of molecular dynamics simulations of pyridine and naphthalene

Simulation cells were constructed by random placement and rotation molecules. This procedure was carried out at low density to reduce the probability of molecular overlap. After an initial energy minimization step to remove any high energy structures formed, the system is allowed to reach

equilibrium density by running an MD simulation in the isobaric-isothermal NPT ensemble. Temperature and pressure were maintained using the Nose-Hoover[i,ii] and Parinello-Rahman[iii,iv] algorithms respectively. The simulation boxes were then scaled to match the density as used in the EPSR simulations and run for at least 5 million time steps (5ns).The GROMACS MD simulation code (v4.6) was used for all simulations[v] using the leap-frog MD algorithm[vi] and the Verlet pair list scheme for neighbor searching[vii]. A time step of 1fs was used for all simulations. Cubic periodic boundary conditions were employed to approximate infinite bulk behaviour. The cut-off of the non-bonded interactions was set at 1nm, with a standard dispersion correction for energy and pressure employed to account for longer range dispersion interactions. Long range electrostatic interactions were dealt with using the Particle Mesh Ewald procedure[viii]. The atom positions for the asphaltene molecules are recorded every 1000 time steps (1ps).

---

[i] Nosé, S. *Mol. Phys.* **1984**, *52*, 255–268.
[ii] Hoover, W. G. *Phys. Rev. A*, **1985,** *31*, 1695–1697.
[iii] Parrinello, M., Rahman, A. *J. Appl. Phys*. **1981**, *52*, 7182–7190.
[iv] Nosé, S., Klein, M. L. *Mol. Phys*. **1983**, *50,* 1055–1076.
[v] Pronk, S. et al. *Bioinformatics*, **2013**, *29*, 845–54.
[vi] Hockney, R.W.; Goel, S. P.; Eastwood, J. *J. Comp. Phys.* **1974**, *14*, 148–158.
[vii] Páll, S., Hess, B. *Comp. Phys. Comm.* **2013,** *184*, 2641–2650.
[viii] Darden, T.; York, D.; Pedersen, L. *J. Chem. Phys.* **1993,** *98*, 10089–10092.